Volume 14, (1995) number 1, pp. 35–46

COMPUTER GRAPHICS *forum*

Image Warping Using Few Anchor Points and Radial Functions

Nur Arad and Daniel Reisfeld

School of Mathematical Sciences, Tel-Aviv University, Tel-Aviv 69978, Israel.
e-mail: nur@math.tau.ac.il, reisfeld@math.tau.ac.il

Abstract

Transformations based on radial basis junctions have proven to be a powerful tool in image warping. In the present work we decompose these transformations into linear and radial terms, and show examples where such a decomposition is advantageous. Locally supported basis functions are introduced. Several applications are demonstrated, and a comparison with other warping techniques is carried out. Finally, some fine points of image warping are discussed.

Keywords: Image warping; radial basis functions; local support; facial expressions; normalization

径向基函数插值

1. Introduction

有界子区域

An image warp is a transformation of a bounded subregion of the plane onto itself with the colour or greyscale associated with each point transformed accordingly. Warping of objects, especially of elastic ones such as human faces, appears in various computer graphics and computer vision applications. These include areas such as image registration (matching of two or more images taken usually by different sensors)[1, 2], computer animation[3,4] and recognition systems, where the warp is used for normalizing the image to some invariant representation prior to recognition or classification[5–7],

Some researchers construct warp models that describe objects in a particular field. We call such an approach *model dependent*, and it is especially used in facial animation[8,9]. The impressive results exhibited by such procedures notwithstanding, realistic modelling of natural objects is extremely difficult, and many different models are needed. As an alternative, *model independent* approaches construct simple, general purpose transformations using no specific information about the object being warped[4,10,11].

模型依赖

The theory of *radial basis functions (RBF)* provides an attractive framework for image warping. Bookstein[12] suggested the use of a subclass of these functions, known as *thin-plate splines*, for image registration purposes since their use minimizes a global measure of the warping the image. However global effects are in many cases undesirable – many objects undergo elaborate transformations which have local, as well as global, components. Previously[13] we introduced RBF based transformations that may be used to emphasize a local influence of the anchor points. Other global constraints are incorporated as well, and tradeoff parameters govern the effect of the various constraints.

Using these transformations in various applications, we have realized that they suffer two drawbacks. All anchor points contribute to the global affine component of the mapping, and all the known radial functions do not have compact support and, therefore, induce some global effect. In the present work we have decomposed the mapping into affine and elastic components. The affine compensates for changes in camera viewpoint, while the elastic simulates intrinsic transformations of the objects, such as a change in facial expression. Although the two components are distinct they are evaluated almost simultaneously, giving rise to a single transformation. This decomposition enables us to define a family of transformations where, if desired, the influence of each anchor point is local.

An important special case arises when the view point is unchanged, in which case the affine component reduces to the identity mapping. Another consequence is the possibility of specifying a minimal number of an-

chor points (one point in an extreme case) rather than at least the three points that were needed previously.

Furthermore, we have found a smooth basis function which has local support. Thus the local influence of each anchor point is absolutely guaranteed. In addition fewer computations are needed, and a weak notion associativity is achieved.

Finally, various applications for facial images are demonstrated.

2. The Mapping

We regard images as *2D* objects. In this respect, an image is a finite domain of a plane with a grey level (or colour) associated with each point. A warping of an image is then primarily a transformation of the plane to itself, and the grey level values are transformed according to the transformation of their associated coordinates. Our main concern is the construction of a mapping of images (planes) that are determined by the mapping of a small number of *anchor points* — points whose mapping is predetermined. This requirement leads us to interpolation theory. 插值理论

2.1. 2D RBF Transformations

In two-dimensional interpolation theory one deals with computing a function $F : \mathbb{R}^2 \to \mathbb{R}$ satisfying 满足

$$F(\bar{x}_i) = \eta_i \quad \text{for} \quad i = 1, 2, \ldots, N.$$

A straightforward generalization of this theory to functions $T : \mathbb{R}^2 \to \mathbb{R}^2$ is interpolation of the form $T(\bar{x}_i) = \bar{y}_i$ for $i = 1,2,\ldots,N$, where $\bar{x}_i, \bar{y}_i \in \mathbb{R}^2$. We define $T : \mathbb{R}^2 \to \mathbb{R}^2$. a 2D *radial basis function transformation*(RBFT) as a transformation of the form

$$T(\bar{x}) = A(\bar{x}) + R(\bar{x}) \tag{1}$$

仿射变换

where $A(\bar{x}) = M\bar{x} + \bar{b}$ is a *2D* affinetransformation (*M* is a *2* x *2* real matrix), and $R(\bar{x})$ is a radial transformation 辐射变换 defined by

$$R(\bar{x}) = (R_X(\bar{x}), R_Y(\bar{x}))$$

R_X and R_Y are both radial functions of the form 径向函数

$$F(\bar{x}) = \sum_{i=1}^{N} a_i g(\| \bar{x} - \bar{x}_i \|) \tag{2}$$

一元函数

$g : \mathbb{R}^+ \to \mathbb{R}$ is a univariate function, termed the radial basis function, and $\| \cdot \|$ denotes the usual Euclidean norm on $\mathbb{R}^2$. 径向基函数 欧式范数

An RBFT is determined by *2(N+3)* coefficients: 6 for the affine part, and *2N* for the radial components; alternatively *N* +3 coefficients are needed to specify the transformation in each coordinate. We define an image-warping transformation based on the mapping of *N anchor points:*

$$T(\bar{x}_i) = \bar{y}_i \quad \text{for} \quad i = 1, 2, \ldots, N \tag{3}$$

where $\bar{y}_i = (y_{i,1}, y_{i,2})$ is the target coordinates of the i'th point. These interpolation conditions translate into *2N* linear equations in the coefficients of the RBFT, thus leaving 6 degrees of freedom (3 for each dimension).

Previously[13,12] two sets of three equations were added in a manner that generalizes affine transformations: The RBFT degenerates to an affine transformation whenever the interpolation conditions allow. The use of the thin-plate spline, $g(t) = t^2 \log t$ (with $g(0) = 0$), as a basis function ensures the minimization of a bending energy functional. In this sense the thin-plate spline is global in nature, and one cannot avoid the global effect of each anchor point. Among others, this means that the transformation of each pixel is affected by each anchor point, which is computationally time-consuming. Lately, an extremely efficient algorithm that computes thin-plate splines on a regular fine rectangular grid (i.e. an image), provided the number of anchors is at least in the hundreds, has been developed by Powell[14].

The use of other basis functions such as the Gaussian $g(t) = e^{-t^2/\sigma^2}$ enables us to incorporate locality constraints by properly tuning the locality parameter σ of each anchor point. A unique solution is guaranteed in case of the thin-plate, the Gaussian, and a few other classes of functions. We shall now consider a different set of Constraints.

2.2. Decomposition of the Transformation

The notation adopted in equation (1) for the RBFT suggests an alternative approach to adding the additional equations: one can simply determine *a priori* the affine component of the RBFT and then solve the interpolation equations subject to these constraints. For example, one can use the identity mapping as the affine component of the RBFT. This corresponds to a situation where the viewpoint is fixed, and all warping is due to a non-rigid transformation of the object, such as a change in its expression.

As another example, one can take the problem of face normalization. As we have demonstrated[15,5], the affine transformation determined by the location of the eyes and mouth is instrumental in face recognition. Thus, one can mark two sets of anchor points. One set (the affine set) determines the affine part of the mapping, while the other set (the radial set) controls the generation of changes in the facial expression. Note that these sets may intersect, and may even be identical.

Controlling the affine component, $A(\bar{x})$, in (1) is carried out according to the number of anchor points in the affine set, as follows. If no points are specified, the affine component is the identity mapping; if one point is specified – translation; two points – translation and scaling; three points – general affine transformation; more than three – general affine transformation determined by a least-square approximation procedure. Alternatively, one can decide that the most general affine mapping admitted is similarity (translation, scaling and rotation), in which case a least-square approximation scheme is needed when the affine set consists of three or more points. The importance of forcing the affine component to being a similarity mapping will be discussed in a later section.

After the affine component, $A(\bar{x})$, has been computed, we turn to determining the radial component, $R(\bar{x})$, in (1). From (1) and (3) it follows that the radial component satisfies:

$$R(\bar{x}_i) = \bar{y}_i - A(\bar{x}_i) \ , \quad i = 1, 2, \ldots, N \tag{4}$$

Since the affine component is determined beforehand, (4) is equivalent to an interpolation problem with *pure radial sums*, i.e. the coefficients a_i of (2) in each of the coordinates (i.e. k = 1,2) are determined by solving the linear system

$$\sum_{j=1}^{N} a_{j,k} g\left(\|\bar{x}_i - \bar{x}_j\|\right) = \\ = y_{i,k} - (A(\bar{x}_i))_k \ \text{ for } \ i = 1, 2, \ldots, N \tag{5}$$

The theory of radial basis functions ensures the solvability of (5) provided the anchor points are distinct. However, the radial basis function, g, has to comply to certain conditions, which we discuss below.

2.3. Choosing the Basis

Any choice of the radial basis function, g, should take into consideration the following points:

1. the equations (4) should always be solvable;
2. the solution should be stable;
3. the run time of the transformation should be short;
4. a tradeoff between global and local effect of the transformation of the anchor points should be established.

Conditions (1) and (2) are met by several families of functions including the Hardy multiquadrics16 $g(t) = (t^2 + c^2)^{\pm\frac{1}{2}}$, and the Gaussians, $g_\sigma(t) = e^{-t^2/\sigma^2}$ provided the number of anchor points does not reach into the thousands17. Locality (condition (4)) can be ensured by using Gaussians with proper σ parameters[18]. However, the Gaussian has infinite support, which means that each pixel is again affected by each anchor point; alternatively, the Gaussian can be approximated by assuming that it vanishes for large arguments. In order to obtain a reasonable approximation, the cutoff points of the Gaussians should take into account the absolute value of the coefficients a_i of equation (2) which are different for each setting of anchor points. Moreover, these coefficients are determined by the Gaussians themselves, thus making a circular dependency. These drawbacks have led us to search for a Gaussian shaped basis function with a compact support.

We have found two families of functions that comply to these constraints:

- the transition function:

$$g_\sigma(t) = \begin{cases} 1 - (t/\sigma)^2(3 - 2t/\sigma) & 0 \le t \le \sigma \\ 0 & t > \sigma \end{cases}$$

- the one-sided cubic spline:

$$g_\sigma(t) = \begin{cases} 6(t/\sigma)^2(t/\sigma - 1) + 1 & 0 \le t \le \frac{1}{2}\sigma \\ 2(1 - t/\sigma)^3 & \frac{1}{2}\sigma < t \le \sigma \\ 0 & t > \sigma \end{cases}$$

Figure 1 (left) shows a plot of these functions together with the Gaussian. The locality parameter σ is used to fulfill requirement (4). They are both fast to compute, especially if look-up tables are used, which is possible due to their compact support. We have not found significant differences in the performance of these two basis functions, although the one-sided cubic spline is smoother (C^2) than the transition function (which is only C^1).

2.4. Solvability and Stability

The question of solvability (condition 1) is subtle. A necessary and sufficient condition for the solvability of an interpolation problem by a pure radial sum in $\mathbb{R}^m$ is that the radial function $g(t)$ have the representation

$$g(t) = \int_0^\infty \Omega_m(tu)\, \alpha'(u)\, du \tag{6}$$

where $\alpha(u)$ is non-decreasing and bounded for $u \ge 0$,

$$\Omega_m(r) = \Gamma(\frac{m}{2})(\frac{2}{r})^{\frac{1}{2}(m-2)} J_{\frac{1}{2}(m-2)}(r)$$

and $J_k(r)$ is the Bessel function of order k[19]. In our case, the dimensionality, m, is equal 2, $\Gamma(2/2) = 1$, and thus

$$\Omega_2(r) = J_0(r) \tag{7}$$

From equations (6) and (7) follows that $g(t)$ must admit to a representation

$$g(t) = \int_0^\infty J_0(tu)\, \alpha'(u)\, du \tag{8}$$

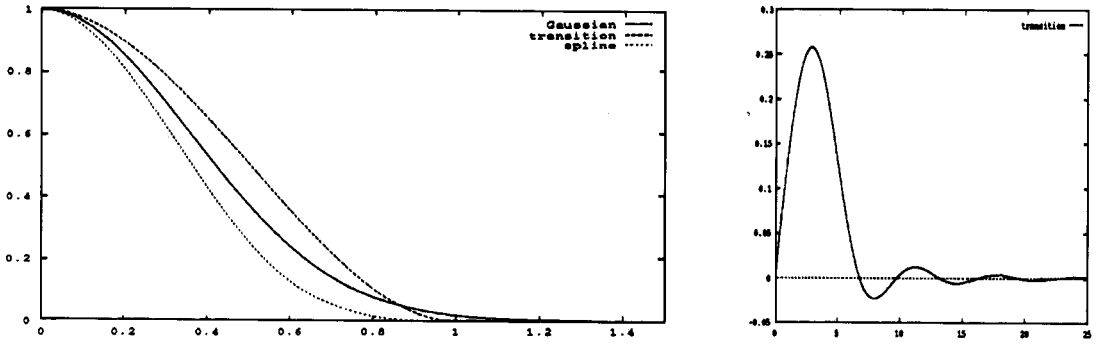

Figure 1: Left: *Plot of the three radial functions with locality parameter discussed in the text. The value* $\sigma = 2$ *was used for the Gaussian.* Right: *Plot of the functions* $\alpha'(u)$ *defined by equation (9) for the transition function.*

In order to compute $\alpha(u)$ we use the Hankel transform pair[20]:

$$F(u) = \int_0^\infty g(t) J_0(ut) t\, dt$$
$$g(t) = \int_0^\infty F(u) J_0(ut) u\, du$$

Identifying the radial basis $g(t)$ with the $g(t)$ in the Hankel transform pair, we obtain

$$\alpha'(u) = uF(u) = u \int_0^\infty g(t) J_0(ut) t\, dt \qquad (9)$$

We have evaluated $\alpha(u)$ numerically for both the transition and the one-sided cubic spline basis functions. In both cases $\alpha(u)$ is bounded, but, unfortunately, is not non-decreasing. Therefore, solvability is not guaranteed for every set of data points. However, we have conducted numerous experiments – always being solvable and stable. Moreover, truncating the Gaussian at any cutoff point results in the same theoretical imperfection, i.e. $\alpha(u)$ is not non-decreasing. Figure 1 (right) shows the plot of $\alpha'(u)$ of equation (9) for the transition function. As can be seen, in this case $\alpha'(u)$ is sometimes negative. The same oscillatory behaviour is exhibited by the other Gaussian shaped compactly supported radials. It is tempting to try to formulate some criteria on the location of anchor points ensuring solvability by looking at the areas where these functions are negative. Unfortunately the connection between solvability and the representation (8) is done through Fourier analysis, thus a constructive connection between the non-positivity of $\alpha'(u)$ and a configuration of anchor points not yielding a unique solution is not possible.

The conclusion from the above discussion is that one can follow two strategies to ensure local effect. The theoretically sound, but time consuming, approach is to use the Gaussian basis with no cutoff. In this case the run time of the computation per pixel is the number of anchor points multiplied by the evaluation time of a Gaussian. One needs a look-up table of the order of the image size in order to avoid direct evaluation of Gaussians. Another drawback of using Gaussians with no cutoff lies in the fact that a truly local effect of an anchor point cannot be achieved. We elaborate on this point by examples in the next section. The second strategy is to switch to a basis function with a compact support. In this case the run time of the transformation per pixel is the number of anchor points whose distance is smaller than the radius of the support. The transition or one-sided cubic splines have a natural cutoff point, suitable for storage in look-up tables (or even direct evaluation); however, like the truncated Gaussian, they do not ensure solvability.

It remains of interest to determine whether there exists a Gaussian-shaped basis function with compact support that ensures solvability for interpolation in $\mathbb{R}^2$ (and $\mathbb{R}^3$). The quarter circle

$$g_\sigma(t) = \begin{cases} 1 - \sqrt{1 - (1 - t/\sigma)^2} & 0 \le t \le \sigma \\ 0 & t > \sigma \end{cases}$$

has local support, is decreasing and ensures solvability by direct numerical evaluation of equation (9). However, this function is not Gaussian-shaped and has a too fast decay rate near the origin. This drawback notwithstanding, we have experimented with this basis function with favourable results provided a larger locality parameter, σ, is used. Our experience shows that using a σ twice as large as the one used for the other compact support basis functions mentioned yields comparable results.

We note that there does not exist a compactly supported radial function that ensures solvability in $\mathbb{R}^n$ for

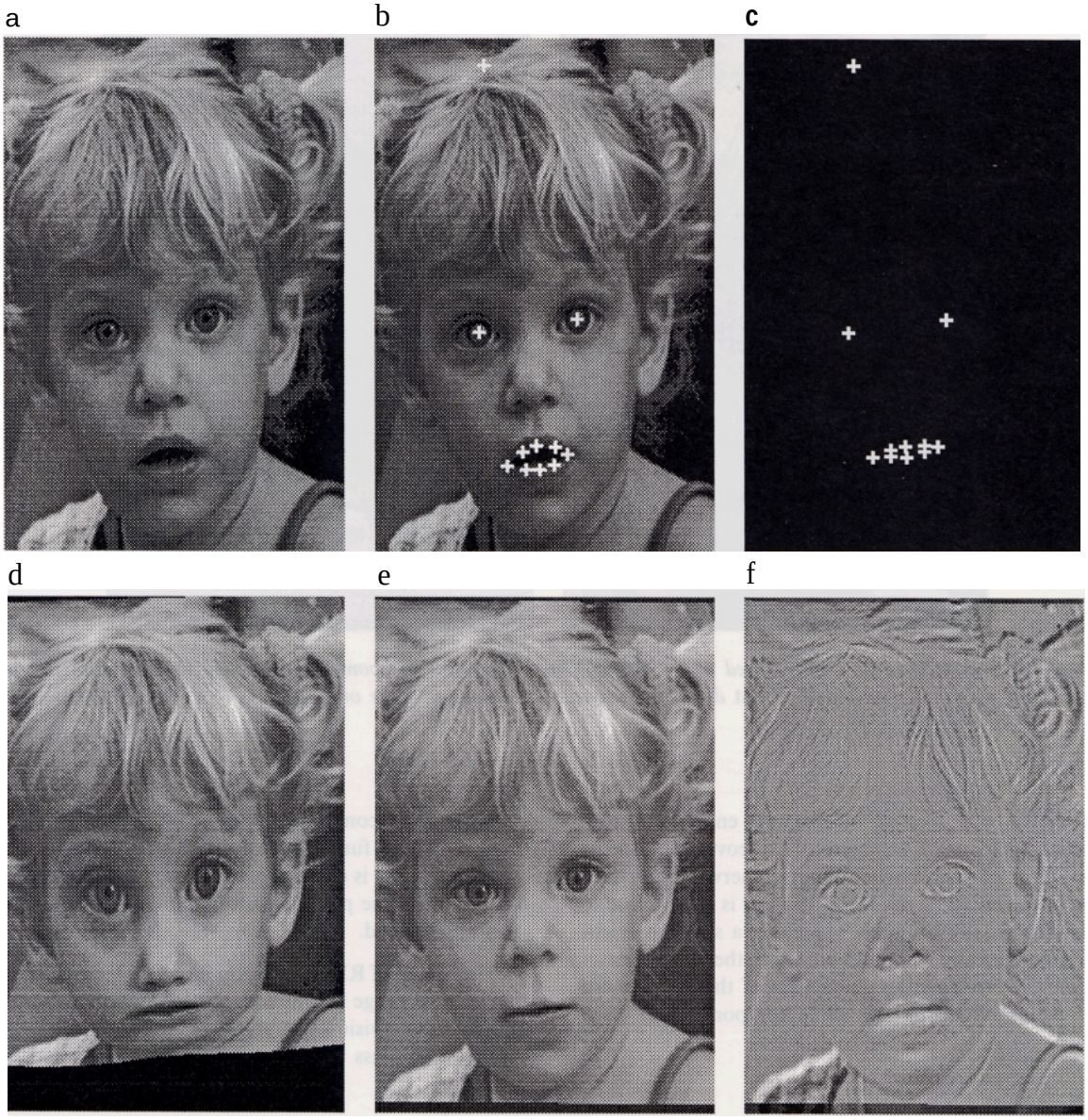

Figure 2: *Unsatisfactory results obtained by using thin-plate splines for animation.* (a) *Original image.* (b) *Source anchors on source image.* (c) *Target anchors on empty image.* (d) *Result of image warp with thin-plate spline.* (e) *Result of warp with Gaussian radial function.* (f) *Difference of* (e) *and* (a) *showing the global nature of the mapping.*

all ***n.*** This is due to the fact that such a function g admits to a representation

$$g(t) = \int_0^\infty \exp(-t^2u^2)\alpha'(u)\,du$$

with $\alpha(u)$ non-negative and bounded[19].Since the exponential is always positive and $\alpha'(u)$ is non-negative, the integral is positive for all t.

The fact that in practice the use of the functions with compact support mentioned results in solvable and stable equations is not accidental. Denote by G the $N \times N$ matrix associated with the left-hand side of equation **(5),** where N is the number of anchor points. Notice that the (i,j)th entry of G is $G_{ij} = g\left(\|\bar{x}_j - \bar{x}_i\|\right)$. Intuitively, G_{ij} measures the effect of the ith anchor point on the transformation at the jth anchor point. It follows

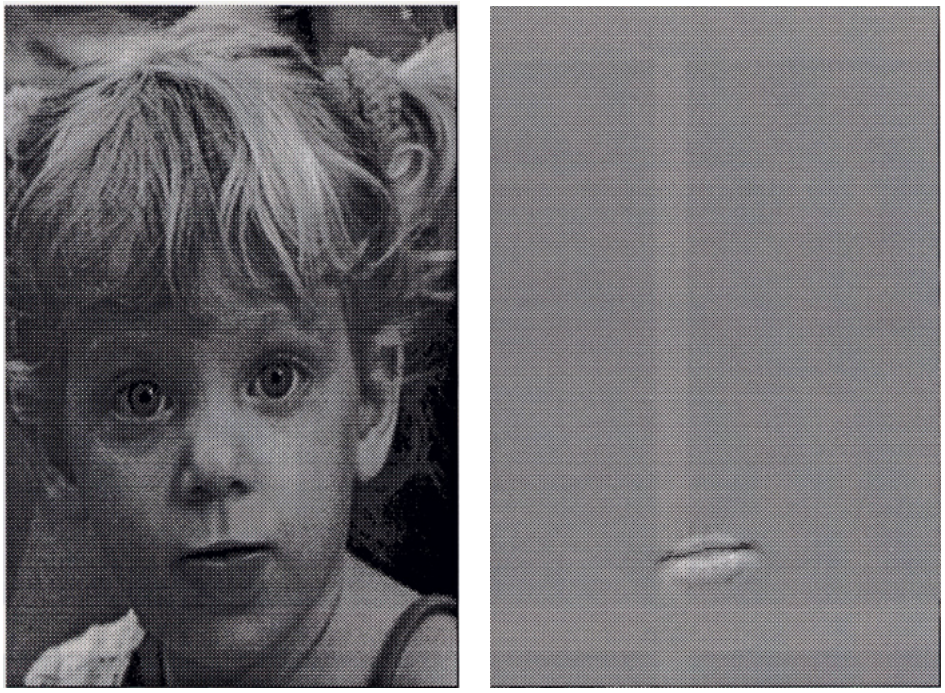

Figure 3: *Same anchors that where used as in Figure 2 but with affine component constrained to unity.* Left: *Output of the warp with Gaussian radial.* Right *difference between left image and the original image (Figure 2a) showing the completely local nature of the mapping.*

that the $G_{ii} = 1$, and all off-diagonal entries are non-negative and smaller than unity. Moreover, due to the local effect of each anchor point (otherwise, the thin-plate basis should be used) G_{ij} for $i \neq j$ is rarely close to unity and usually vanishes. Therefore, a solution exists, and is numerically stable. In addition, the solvability of equation (5) ensures the uniqueness of the RBFT once the scheme of setting the affine component has been chosen.

3. Applications

We first demonstrate a situation where the use of thin-plate splines and the procedure outlined in Section 2.1 yields unsatisfactory results.

As can be seen in Figure 2, the use of thin-plate splines for animation purposes is unsatisfactory; interpolation with thin-plates emphasizes the global nature of the mapping (since a global warping criteria is minimized). The use of the Gaussian radial function improves the situation. However, as can be seen in the example, some anchors are needed to overcome the strong shearing effect (realized through the affine component which is calculated together with the radial term). In Figure 3 the same anchors and locality parameter σ were used, but the affine component was preset to unity, and the transition basis function was used. The truly local nature of the mapping is clear. Moreover, the top three anchors do not affect the parameters of the mapping and can in fact be excluded.

The family of RBF transformations we have presented has a wide range of applications in computer graphics and computer vision. We present examples from various fields and discuss the fine points in the application.

3.1. Modifying Facial Expressions and Features

The power of the decomposition of the affine and elastic components of the transformation is best demonstrated by the application of the transformation using only *one* anchor point. Since no points are specified for the affine component of the RBFT, it is taken as unity. Figure 4 shows the outcome of such a transformation. We remark that previously the same effect was achieved[13], but with the use of six anchor points, which results in a considerable increase in run time. In addition, five of the six anchor points functioned as fixed points, and the actual warp was driven by the displacement of one point. Thus, most of the points were used to overcome a

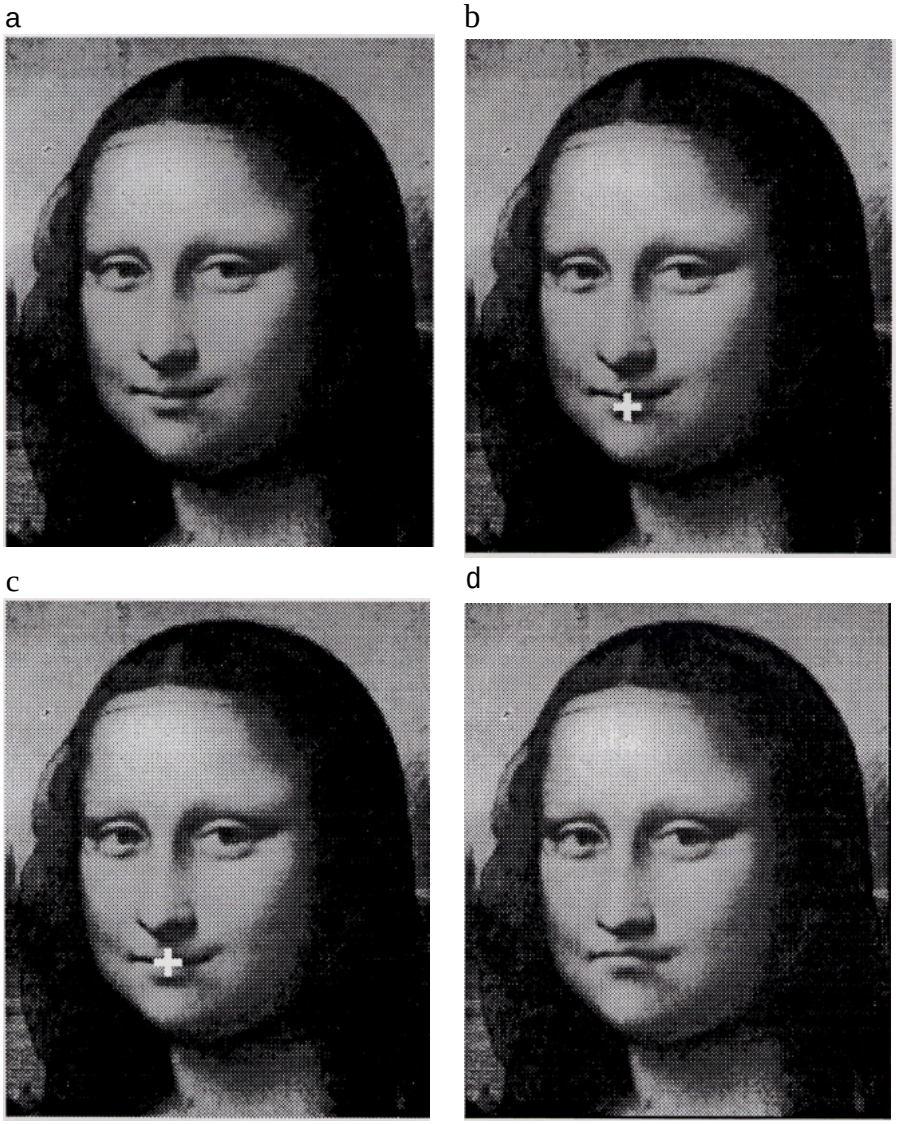

Figure 4: *An RBFT using one anchor point. (a) Original image. (b) Source anchor point marked. (c) Position of target anchor point marked. Note that the image itself is used only for reference. (d) Outcome of the one-point warp. The locality parameter σ was set at about 1/2 the distance between the eyes.*

technical shortcoming in the structure of the transformation. The decomposition of the mapping into affine and elastic components enables to overcome this disadvantage.

Figure 5 shows the application of RBFT in modifying facial features. Since the features modified are local in nature, the decomposition of the transformation into global (affine) and local (radial) components is crucial. The straightening of the brow has an effect on the eye, thus some anchor points were used to fix the eye in place. Notice that the feature modification of the ear (clipping or shortening) is of a different nature than that of the brow (modification of the angle).

3.2. Normalization of Faces for Recognition

In the previous examples only one image was used, and the target anchor points were marked on a copy of the source image. There was no need to generate the expression induced by a different image. When dealing with face recognition one needs to cope with a wide

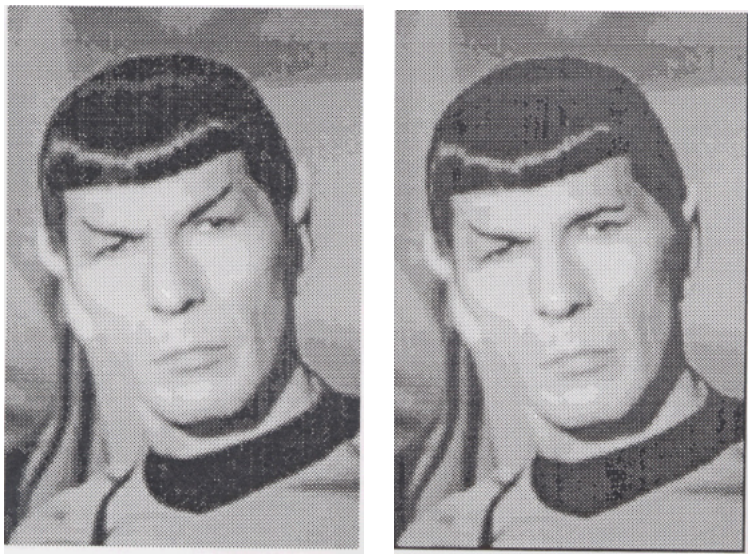

Figure 5: *Humanizing Vulcanfacial features.* Left: *original image of a typical Vulcan.* Right: *output of the transformation. 8 anchor points were used around the right eye and an additional 5 were needed for the right ear. The locality parameter* σ *was set at about 1/3 the length of the eye.*

range of facial expressions and ideally one wishes to be able to transform the image from one expression to another.

A major motivation in the development of RBFT's is successful application of affine transformation for facial normalization. Affine mappings are first-order approximations suited for overcoming changes in an image due to different camera viewpoints. These mappings however cannot overcome changes in facial expressions. Figure 6 shows the application of an RBFT on an image in order to compensate for differences in the facial expressions of the source and target images. Figure 6(f) shows that a global strategy is ineffective in such a case.

A different strategy useful in face normalization is the application of RBFT's on two images with target anchor points being the average of the source anchor points of both source images. Such a procedure is depicted in Figure 7.

4. Discussion

4.1. Comparison with other Works

In the last several years a vast amount of research has been directed towards animation of facial expressions. From our point of view models and procedures intended at facial animation may be classified into two families: the first (model dependent) generate facial expressions by first constructing a mathematical model of the physical face, and then defining the dynamics which govern the non-rigid motion of the object[9, 8]. These techniques may exhibit impressive results, but suffer from the fundamental drawback that they are object dependent, i.e. a different model is needed for different non-rigid objects. The second family of techniques (model independent) simulate deformations without using any information on the object being deformed[11, 21,22]. Recently these two approaches have been combined[23], in the sense that an association between mathematical parameters defining the transformations and real-life facial expressions was established, giving rise to an expression editor.

The present work falls within the category of model independent transformations. The user has to specify the position of the source and target anchors. Of crucial importance in our model is the relatively small number of points needed in order to define the warp, with even the extreme case of one anchor point (as in Figure 4) possible. By contrast, another model that defines a transformation by the position of anchor points is the *free-form deformation* model of Sederberg and Parry[11], however the anchors (control points) must lie on a regular grid, thus imposing at least eight control points, and typically many more. Moreover, the position of the points may not coincide with the position of physical features that are to be manipulated. Another algorithm that has cumulated in an impressive Michael Jackson video is the *feature based image metamorphosis* algorithm[4], where the position of each point is the weighted average of affine transformations determined by corresponding line

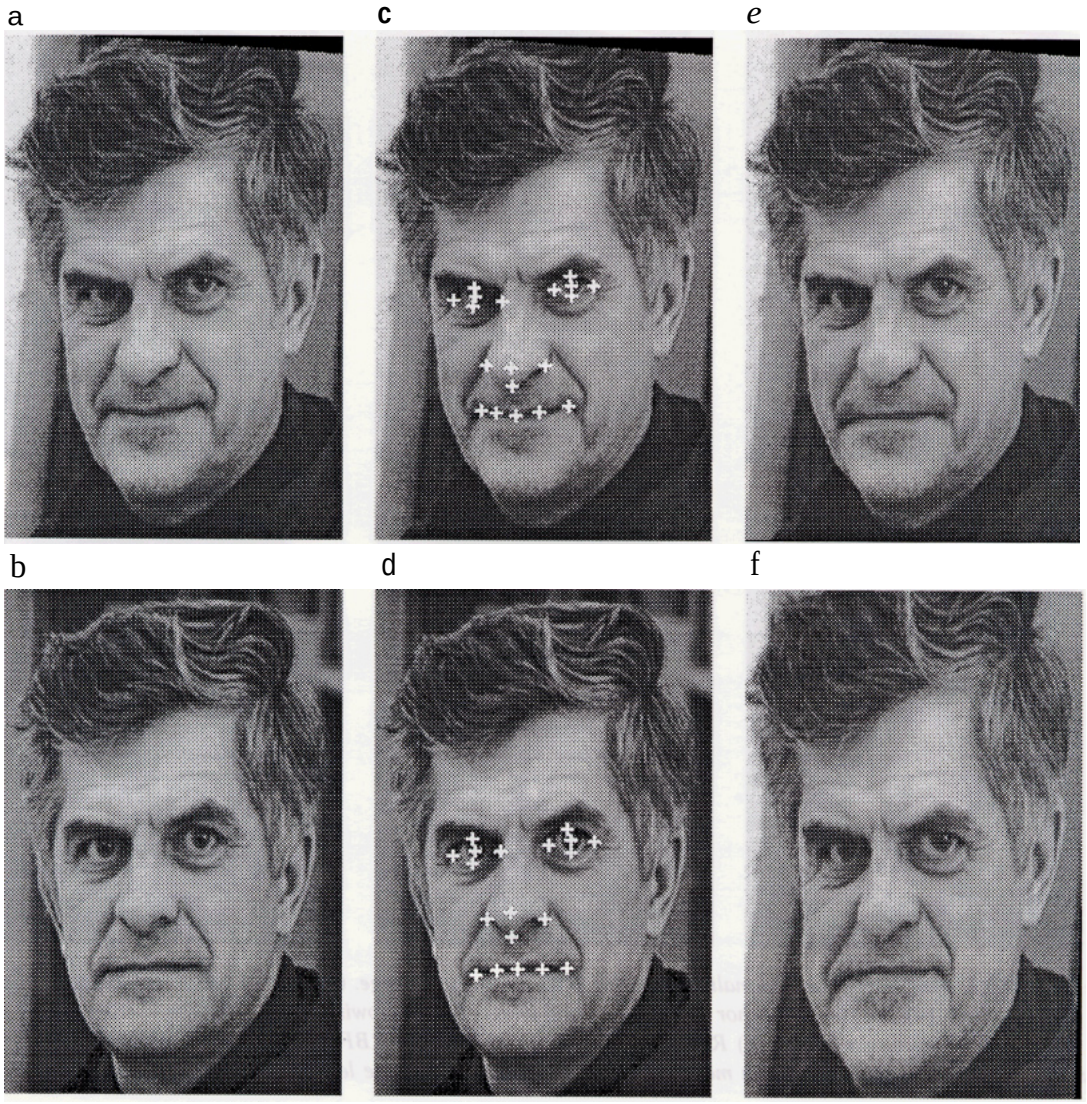

Figure 6: *Facial normalization using RBFT.* (a) *Original source image.* (b) *Target image.* (c) *Position of source anchor points marked.* (d) *Position of target anchor points.* (e) *RBFT applied. The affine component was unity, transition radial function used with* σ *equal to* 1/2 *the length of the eye.* (f) *same anchor points used but with a thin-late spline minimizing the bending energy of the transformation. Notice the global effects which overshadow the local changes desired.*

segments in the source and target images. Since each line segment corresponds to two points, this mapping needs at least four anchor points in order to generate non-linear warps. In addition, since in the original formulation of the algorithm segments cannot intersect, not every configuration of anchor points is possible. Finally, the weight functions governing the effect of each segment on the mapping are not local, thus each pair of anchors has a global effect. This last point may be modified by using locally supported weight functions.

4.2. 2D Versus 3D

The theoretical discussion and the examples shown are all two-dimensional. These simulate the transformations that three-dimensional objects undergo. The reduction from three to two dimensions is first and foremost attractive from the computational complexity point of view. Moreover, there is psychophysical evidence suggesting that two-dimensional representations are used by biological visual systems in recognition[24,7].

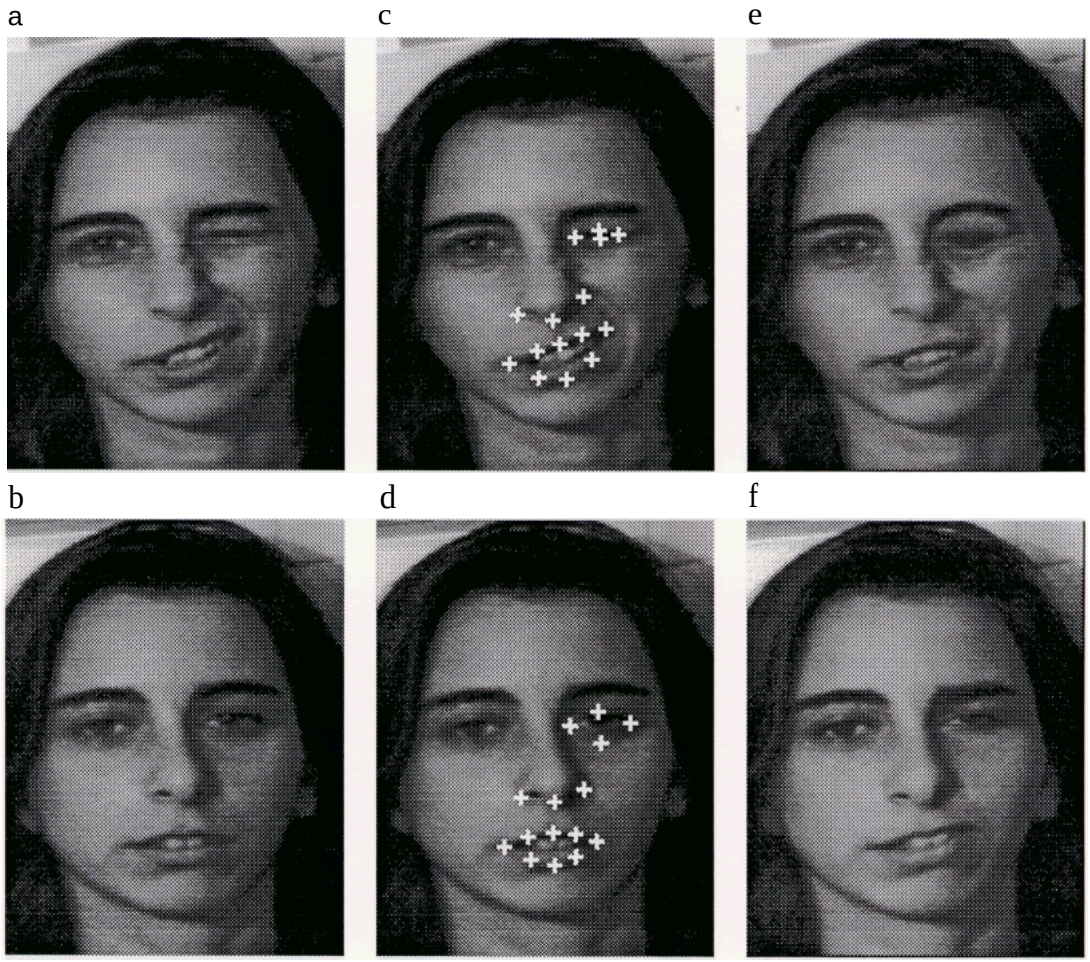

Figure 7: *Another example of facial normalization using RBFT.* (a) *First image.* (b) *Second image.* (c) *Position of anchor points on first image.* (d) *Position of anchor points on second image. Both following warps used the average of the anchor points of* (b) *and* (c) *as target points.* (e) *RBFT on first image applied.* (f) *RBFT on second image applied. Notice that expressions of the right images are much more similar to one another than the left-hand expressions.*

There is no difficulty in applying the technique to three-dimensional objects. In this case the decomposition of the transformation into affine and radial components may prove quite useful due to the fact that rigid movement, both of the object and the viewpoint, translate to orthogonal affine mappings which are computed before the elastic (radial) component is determined.

4.3. Composition of RBFT's and Group Structure

One feature of affine mappings is their group structure; the family of affine transformations is closed under composition and inversion. This structure is attractive in interactive systems, since the position of the anchor points can be successively tuned. Thus, the final outcome is memoryless. The family of RBFT generalize affine transformations in various respects, but the group structure is destroyed. However, due to the decomposition of the RBFT into affine and elastic components, and due to the use of basis functions with compact support it is possible under certain conditions to compose and invert RBFT's. Specifically, the family of RBFT's commutes with isometry mappings, and with similarity mapping provided the locality parameter, σ, is scaled according to image size. The composition of two RBFT's is equivalent to an RBFT that is determined by the total displacement provided the anchors' influences do not intersect. In practice, since overlap is small, the differences between composition and one-shot are quite small.

In addition we have found that in many cases although a shear factor is present in an affine component,

for mild shears there is no noticeable difference between the two transformations. Invariance under scaling is also important from the numerical point of view; with the increase in the number of anchor points the linear systems involved may become highly ill-conditioned25 and scaling the image to fit into the unit square is known to reduce the condition number of the system.

Acknowledgments

This research resulted from a consulting job for Scitex Corporation. We thank Amir Kaplan and Shay Zamir for their cooperation. Many thanks to Yehezkel Yeshurun for his deep insight, especially with regards to non-linear warps.

References

1. J. Flusser, "An adaptive method for image registration," *Pattern Recognition,* 25 pp. 45–54 (1992).
2. M. Moshfeghi, "Elastic matching of multimodality medical images," *CVGIP: Graphical Models and Image Processing,* 53(3), pp. 271–282, (1991).
3. M. Oka, K. Tsutsui, A. Ohba, Y. Kurauchi, and T. Tago, "Real-time manipulation of texture mapped surfaces," *Computer Graphics,* 21(4), pp. 181–188, (1987).
4. T. Beier and S. Neely, "Feature-based image metamorphosis,'' *Computer Graphics,* 26(2), pp. 35-42, (1992).
5. S. Edelman, D. Reisfeld and Y. Yeshurun, "Learning to recognize faces from examples," In *Proceedings of the 2nd European Conference on Computer Vision,* pp. 787–791, Santa Margherita Ligure, Italy, May 1992.
6. D. Reisfeld and Y. Yeshurun, "Robust detection of facial features by generalized symmetry," In *Proceedings of the 11th International Conference on Pattern Recognition,* The Hague, Netherlands, September 1992.
7. D. Reisfeld, *Generalized symmetry transforms: attentional mechanisms and face recognition,* PhD thesis, Tel-Aviv University, January 1994.
8. D. Terzopolous and K. Waters, "Physically based facial modeling, analysis, and animation," *Journal of Visualization and Animation,* 1(2), pp. 73–80, (1990).
9. F. I. Parke, "Parameterized models for facial animtion," *IEEE Computer Graphics and Applications,* pp. 61–68, November 1982.
10. G. Wolberg and T. E. Boult, "Separable image warping with spatial lookup tables," *Computer Graphics,* 23(3), pp. 369–378, (1989).
11. T. W. Sederberg and S. R. Parry, "Free-form deformation of solid geometric models," In *SIGGRAPH '86,* pp. 151–160 (1986).
12. F. L. Bookstein, "Principal warps: Thin-plate splines and the decomposition of deformations," *IEEE Transactions on Pattern Analysis and Machine Intelligence,* 11, pp. 567–585, (1989).
13. N. Arad, N. Dyn, D. Reisfeld and Y. Yeshurun, "Image warping by radial basis functions; application to facial expressions," *CVGIP: Graphical Models and Image Processing,* (1994, in press.).
14. M. J. D. Powell, "Tabulation of thin plate splines on a very fine two-dimensional grid," Technical Report DAMTP 1992/NA2, Numerical Analysis Reports, University of Cambridge, 1992.
15. D. Reisfeld, H. Wolfson and Y. Yeshurun, "Detection of interest points using symmetry," In *Third International Conference on Computer Vision,* pp. 62–65, Osaka, Japan, December 1990.
16. R. L. Hardy, "Multi quadratic equations of topography and other irregular surfaces," *Journal of Geophysical Research,* 76, pp. 1905–1915, (1971).
17. N. Dyn, "Interpolation and approximation by radial and related functions," In C. K. Chui, L. L. Schumaker and J. D. Ward, editors, *Approximation Theory VI,* volume 1, pp. 211–234. Academic Press, (1989).
18. G. A. Micchelli, "Interpolation of scattered data: distance matrices and conditionally positive definite functions," *Constructive Approximation,* 2, pp. 11–22, 1986.
19. I. J. Schoenberg, "Metric spaces and completely monotonic functions," *Annals of Mathematics,* 39, pp. 811–841, (1938).
20. B. Davies, *Integral Transforms and their applications,* Springer-Verlag, (1978).
21. Z. C. Li, C. Y. Suen, T. D. Bui and Q. L. Gu, "Harmonic models of shape transformations in digital images and patterns," *CVGIP: Graphical Models and Image Processing,* 54(3), pp. 198–209, May 1992.
22. C. Frederick and E. L. Schwartz, "Conformal image warping," *IEEE Computer Graphics and Applications,* March 1990, pp. 54–61, (1990).
23. P. Kalra, A. Magnili, N. Magnenat Thalmann and D. Thalmann, "Simulation of facial muscle actions based on rational free form deformations," *Computer Graphics Forum,* 11(3), C–59 – C–69, (1992).

24. H. H. Bülthoff and S. Edelman, "Psychophysical support for a 2D view interpolation theory of object recognition," *Proceedings of the National Academy of Sciences,* 89, pp. 60–64 (1992).

25. I. Barrodale, D. Skea, M. Berkley, R. Kuwahara and R. Poeckert, "Warping digital images using thin-plate splines, *Pattern Recognition,* 26(2), pp. 375–376 (1993).